Polyhydroxyurethane Covalent Adaptable Networks: Looking for Suitable Catalysts

Camille Bakkali-Hassani, Dimitri Berne, Pauline Bron, Lourdes Irusta, Haritz Sardon, Vincent Ladmiral, Sylvain Caillol

Polyhydroxyurethane Covalent Adaptable Networks: Looking for Suitable Catalysts

Camille Bakkali-Hassani*,[a] Dimitri Berne,[a] Pauline Bron,[a,b] Lourdes Irusta,[b] Haritz Sardon,[b] Vincent Ladmiral [a] and Sylvain Caillol*[a]

Abstract: Various bases (DMAP, DBU, TBD, *t*-BuOK), acid (*p*-TSA), thiourea (TU) and organometallic Lewis acid (DBTDL) were investigated as potential catalysts for the preparation of polyhydroxyurethane covalent adaptable networks. Catalytic systems were first selected for their ability to promote cyclic carbonate aminolysis quantitatively (full conversion of cyclic carbonates) with few or no side reactions (urea formation). Selected PHU networks were extensively characterized using thermo-mechanical analysis (TGA, DSC, DMA and tensile test), rheology experiments (stress relaxation, frequency sweep), spectroscopy analysis (ATR-IR), swelling and reprocessing tests. Combining rheology, ATR-IR analysis and model molecular reactions, we suggest a catalyst-dependent exchange mechanism in which solely the organotin Lewis acid (DBTDL) was capable to promote transcarbamoylation in PHU efficiently with both secondary (major product of aminolysis) and primary alcohols and thus an efficient reprocessing.

Introduction

Polymers have revolutionized our daily life during the last century and are today ubiquitous and irreplaceable in a wide range of applications. The use of petrochemical-based precursors associated with long-termed (bio)degradability and a poor global waste management make also polymers one of the major ecological concerns of our time.[1,2] Designing sustainable polymeric materials prepared from renewable resources and capable of inherent reprocessability, recyclability and degradability appear necessary to address the current environmental challenges.[3–6] The case of polyurethanes (PUs) is a typical example of the challenges polymer chemists face to reach such an ideal and economically viable polymer conception. Industrially, PU-based materials are prepared by reacting toxic isocyanates (prepared from phosgene) and polyols in a polyaddition process catalysed by toxic organotin catalysts.[7] Moreover, roughly sixty percent of the annual global production (which represent more than 12 Mt/year) are PU thermosets, *i.e.* permanently crosslinked networks, non-recyclable and non-reprocessable materials.[8,9]

Polyhydroxyurethane (PHU) chemistry and derivatives have been extensively studied to replace PU produced from isocyanate monomers in the so-called non-isocyanate polyurethane (NIPU) strategy.[10,11] In classical PU chemistry, carbamates are generated by isocyanate alcoholysis whereas hydroxyurethane moieties result from the ring-opening of cyclic carbonate (CC) by primary amine. This approach brings several advantages such as the use of non-toxic and user-friendly monomers generated from CO_2 and epoxides, high stability (isocyanate reacts with nucleophiles such as water, alcohols, etc.) and compatibility with green chemistry principles.[12–15] However, despite their elegant and green synthesis, PHUs exhibit synthetic drawbacks which hinder their industrial application.[16] The main limitation is the relatively low reactivity of bis-5-CC towards aminolysis, the reversibility of carbonate aminolysis, the occurrence of side reactions (mainly urea formation) and the formation of a dense hydrogen bond networks which were shown to limit the conversion and consequently the molar masses of such linear polymers.[16] To increase the reactivity of cyclic carbonates towards aminolysis, different strategies have been explored such as increasing the CC ring size or installing electron-withdrawing substituent on the heterocycle.[17–19]

For thermoset application and especially for the design of dynamic covalent networks (CANs), two distinct exchange mechanisms are commonly admitted to occur in PU and PHU crosslinked networks.[20] On the one hand, associative transcarbamoylation, also called transurethanisation, is the exchange reaction between carbamate linkages and free-hydroxyl groups (Scheme 1a). On the other hand, dissociative transcarbamoylation can occur through two mechanisms depending on the presence of free-hydroxyl groups at specific position along the polymer backbone. In PU-CANs, as no free-hydroxyl groups are available, it is the retro-formation of isocyanate and alcohol moieties which confer dynamic properties to PU network. In PHU-CANs, it is the retrocyclisation of hydroxyurethane moiety which yield to primary amine and cyclic carbonate that has been put forward to explain the dynamic exchange occurring in 5CC-PHU covalent adaptable networks (Scheme 1b).[21] Often described as sluggish, transcarbamoylation (whether associative or dissociative) is known to occur in both PU and PHU networks at relatively high temperature ($T \geq 120°C$), with or without the addition of an exogenous catalyst.[20] Due to a relatively poor control (side reaction observed at high temperature and slow processes), polymer chemists have first set aside those reactions to focus on introducing various dynamic covalent bonds into PHU crosslinked networks.[22] Nonetheless, reprocessable PHUs based on transcarbamoylation *via* reversible cyclisation have been obtained from CC of different ring-size (from 5 to 8).[23–25] In the particular case of 5-CC monomers, the retro-formation of primary amine and cyclic carbonate was first considered as a limitation, as side reactions leading to a decrease in crosslink density were detected.[22] Torkelson and co-workers, by judiciously selecting non-volatile primary amine monomers and an organocatalyst (4-(dimethylamino) pyridine, DMAP), were able to produce PHU-CAN with good reprocessability at moderate temperature (120°C).[21,26–28] Apart from DMAP-based polyhydroxyurethane CANs (and two studies on PU network[29,30]), investigations on suitable catalysts, *i.e.* able to efficiently catalyse both aminolysis and transcarbamoylation with low level of or no side reactions, towards the control of covalent exchange properties (dissociative/associative mechanism) are still lacking.

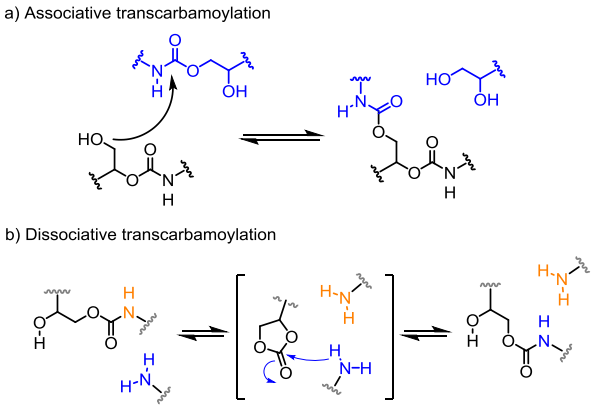

Scheme 1. a) Associative and b) dissociative transcarbamoylation mechanism suggested for PHU covalent adaptable networks.

Herein, we studied the influence of catalysis in PHU covalent adaptable networks to determine its effect on both network formation (kinetic and side reaction) and final material properties. A catalyst selection was first performed by following the aminolysis of cyclic carbonate and the occurrence of side reactions (urea formation) by ATR-IR spectroscopy during and after the curing process at 80°C. Rheological analysis (frequency sweep and stress relaxation) combined with reprocessing test highlighted that only one candidate (a tin-based catalyst) was able to catalyse efficiently transcarbamoylation. ^{1}H NMR kinetic experiments on model molecule combined with rheology experiments (stress relaxation and frequency sweep) and ATR-IR spectroscopy analysis suggested that the rate and the mechanism of exchange was influenced by both the catalyst and alcohol nature (primary *vs* secondary).

Result and discussion

Influence of catalyst on network formation

Polyhydroxyurethane networks were prepared by aminolysis of a tri-functional 5-CC monomer namely trimethylolpropane triglycidyl carbonate (TMPTC, obtained by epoxy carbonation with CO_2 as previously described[36]) with a commercially available bifunctional primary amine namely 4,9-Dioxa-1,12-dodecanediamine (DD) (Figure 1.a). Representative organic acid *p*-toluene sulfonyl acid (p-TSA), thiourea (TU, 1-(3,5 bis(trifluoromethyl)phenyl)-3-cyclohexylthiourea), bases such as 1,5,7-triazabicyclo[4.4.0]dec-5-ene (TBD), 1,8-diazabicyclo[5.4.0]undec-7-ene (DBU), potassium *tert*-butoxide (*t*-BuOK), 4-(dimethylamino) pyridine (DMAP) and organometallic Lewis acid catalyst (dibutyltin(IV)dilaurate, DBTDL) were selected to investigate their ability to promote both network formation (aminolysis) and exchange reaction (transcarbamoylation/retrocyclisation).

Prior to study the influence of the catalyst in PHU formulations, the initial ratio of primary amine/5-CC ($[NH_2]_0/[5\text{-}CC]_0$) was optimized in non-catalysed formulations to ensure complete conversion of cyclic carbonate (Table 1 and Figure S1). A slight excess of primary amine (1 mol%) was found necessary to reach full conversion of the cyclic carbonate. However, increasing this initial ratio leads to the formation of urea (by reaction of free primary amine with urethane moieties) easily discernible in ATR-IR spectra at 1650 cm^{-1} when $[NH_2]_0/[5\text{-}CC]_0 \geq 1.05$ (Figure S1). The initial ratio $[NH_2]_0/[5\text{-}CC]_0 = 1.01$ was thus fixed for all the following experiments.

The catalyst activity towards the aminolysis of cyclic carbonate was investigated by monitoring the curing process at 80°C using ATR-IR spectroscopy. Conversions were calculated following the simultaneous disappearance of $\nu_{C=O}$ carbonate vibration band at ~1780 cm^{-1} and the appearance of urethane-carbonyl vibration band at ~1680 cm^{-1} (Figure 1.b and 1.c). The relative rate constants of catalysed (cat.) and non-catalysed (NC) polymerisation (k_{cat}/k_{NC}) were obtained by plotting $\ln([5\text{-}CC]_0/[5\text{-}CC]_t)$ *vs.* time (Figure S2, Table 1) and allowed the distinction of two catalyst groups (assuming a first order kinetic). Only time points corresponding to the initial rate of the reactions were considered (conversion < 50 %) for the determination of the rate constants. On one hand, in the presence of DMAP or *t*-BuOK, aminolysis rates were comparable to that of non-catalysed (NC) formulations (Figure 1.c), thus demonstrating a low catalytic activity. In the case of *t*-BuOK, the poor dispersion quality (catalyst solid particles were visible to the naked eyes) could also explain the low impact of this catalyst on the aminolysis rate. On the other hand, *p*-TSA, DBTDL, TBD, DBU and TU significantly accelerated the ring-opening reaction at the early stage of polymerisation (from 0 to 5 min). In any case, after 10 min at 80 °C, catalysed and non-catalysed curing exhibited roughly the same conversion profile meaning that the polymerisation process tends to be limited by the diffusion of reactive species (zero-order kinetic profile). All formulations were maintained at 80°C for 24h to ensure high conversion (> 90%).

Apart from these kinetics considerations, discrepancies also arose between samples and in particular regarding the presence/absence of urea detected in ATR-IR spectra at 1650 cm^{-1} (Table 1 and Figure S3) in the fully cured material. Strong bases such as TBD or DBU (pKa = 26.0 and 24.3 respectively in acetonitrile[31]) appeared to favor the formation of urea probably because of the strong amine activation by such organocatalysts (Scheme 2c). This effect was particularly striking for TBD-based materials in which the intensity of the urethane carbonyl stretching observed in ATR-IR spectrum was even lower than the one from urea (Figure S3). With linear PHU, TBD was also reported to unexpectedly catalysed the formation of segmented polyurea-urethane[32] and can be therefore considered as non-suitable for PHU-CAN preparation (starting from 5-CC monomers). Alternatively, TBD was also shown to activate carbamate groups through an acyl intermediate depicted in Scheme 2.d.[33] In contrast, mild bases such as DMAP or *t*-BuOK (pKa = 18.0 and 17.1 respectively[34]) did not lead to side reactions under these conditions. In the presence of electrophile activators such as TU, DBTDL or *p*-TSA, polymerisation rates were higher than for the non-catalysed process and no-or only small quantities of urea bond were detected at the end of the synthesis. Contrary to the base-catalysed mechanism (Scheme 2a), acid activates preferentially the carbonyl group of 5-CC (Scheme 2b) thus limiting undesired side reaction (*e.g.* formation of urea displayed in Scheme 2c). DBTDL due to its Lewis acid character also increased the aminolysis reaction rate following the same activation pathway on the carbonyl group (Scheme 2b). Following these results based on the reactivity towards aminolysis, the strong bases (TBD and DBU), despite their good activity, were put aside because of their tendency to promote urea formation. Catalyst-free PHU network as well as those containing DBTDL, TU, *p*-TSA, *t*-BuOK and DMAP were selected for the rest of the study.

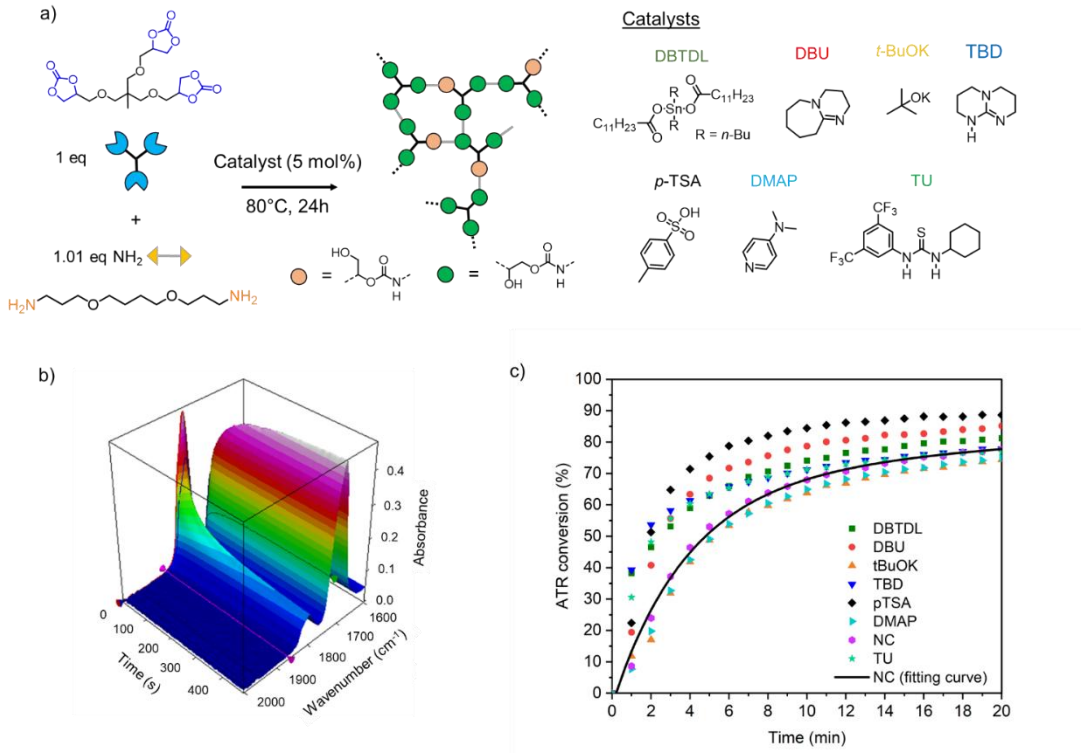

Figure 1. a) Catalytic systems studied for catalysed-PHU network synthesis by reacting TMPTC and DD at 80°C for 24h, b) Evolution of the ATR-IR signals between 2000 and 1600 cm^{-1} as a function of time at 80°C (1 spectrum per minute). Characteristic bands of cyclic carbonate (~1780 cm^{-1}) and urethane (~1680 cm^{-1}). c) ATR conversion calculated using the disappearance of the carbonate signal at 1780 cm^{-1} with different catalysts.

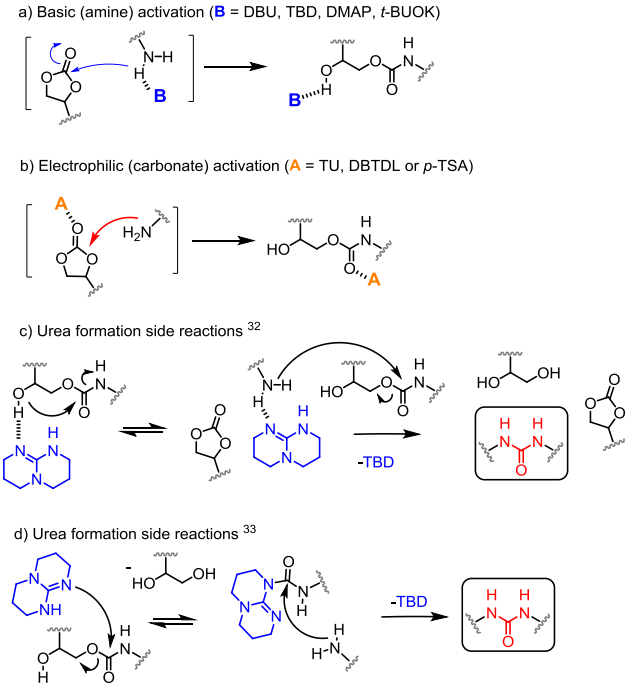

Scheme 2. a) Basic activation of amine and b) Electrophilic activation of carbonate by acids for cyclic carbonate aminolysis c) Proposed mechanism for TBD-catalysed urea formation from hydroxyurethane moieties [32] and d) from carbamate activation [33]

The formation of a chemically crosslinked network was assessed *via* swelling experiments (in DMF at 80°C for 24h). Regardless of the catalyst employed, gel contents were ≥ 85 % for all the samples. The swelling values also show no relationship neither with the conversion nor the urea formation. This is surprising knowing the fact that side reactions leading to urea formation were detected in DBU or TBD-based systems, the latter exhibiting slightly lower swelling index but not significant.

Table 1. PHU formulations studied (5 mol% catalyst, 80°C, 24h)

Catalyst	$[NH_2]_0/[5\text{-}CC]_0$	k_{Cat}/k_{NC} [a]	Urea? [b]	Swelling Index (%)[c]	Gel content (%)[c]
none	1.00	*n.d.*	low	*n.d.*	*n.d.*
none	1.01	1.00	low	218 ± 1	91 ± 0.5
none	1.02	*n.d.*	medium	*n.d.*	*n.d.*
none	1.05	*n.d.*	high	*n.d.*	*n.d.*
p-TSA	1.01	2.65	low	230 ± 14	92 ± 1
DMAP	1.01	0.82	low	213 ± 5	90 ± 2
TU	1.01	2.58	low	245 ± 2	89 ± 3
DBU	1.01	1.96	medium	240 ± 10	85 ± 1
TBD	1.01	3.19	high	198 ± 2	87 ± 1
t-BuOK	1.01	0.78	low	230 ± 15	93 ± 0.5
DBTDL[d]	1.01	2.72	low	226 ± 2	86 ± 0.5

[(a)] Relative polymerisation rate constant (normalized by non-catalysed polymerisation constant rate) and measured from $\ln([5\text{-}CC]_0/[5\text{-}CC]_t)$ *vs* time plot presented in Figure S2 [(b)] Residual Cyclic carbonate and urea bonds content were evaluated using ATR-IR spectroscopy [(c)] Measured after immersion in DMF at 80°C for 24h [(d)] DBTDL is used at 2 mol%; *n.d. = not determined*

Thermo-mechanical characterization of PHU from selected catalysts

The thermo-mechanical properties of the PHU network (non-catalysed or catalysed with DBTDL, TU, *p*-TSA, *t*-BuOK, DMAP) were measured by combining TGA, DMA, DSC and

tensile test experiments and compared to evaluate the effect of the catalyst. Results are summarized in Table 2.

Table 2. Thermo-mechanical properties of selected PHU networks.

PHU	T_g [a] (°C)	$T_{d\,5\%}$ [b] (°C)	G' (MPa)[c] at 80°C	Young modulus [d] (MPa)	Stress at break [d] (MPa)	Strain at break [d] (%)
DBTDL	10	267	0.44	2.0 ± 0.2	0.53 ± 0.10	35 ± 3
TU	10	256	0.34	2.7 ± 0.5	0.52 ± 0.06	28 ± 2
DMAP	11	285	0.26	3.8 ± 0.1	0.97 ± 0.08	33 ± 4
p-TSA	9	276	0.40	3.3 ± 0.5	0.72 ± 0.08	30 ± 3
t-BuOK	9	287	0.25	5.9 ± 0.3	0.96 ± 0.06	24 ± 1
NC	8	283	0.26	3.5 ± 0.4	0.79 ± 0.06	30 ± 4

[(a)] Measured by DSC (second heating curve) [(b)] measured by TGA [(c)] G' (shear modulus) was measured by frequency sweep experiments at 80° [(d)] calculated from tensile test experiments.

All networks demonstrated almost similar thermal stability (256°C ≤ $Td_{5\%}$≤ 286°C) and only slight differences were noticeable between their respective thermograms (Figure S4). Differential scanning calorimetry (DSC) analyses showed, once again, that the catalysts did not affect the glass transition temperatures (T_g) which were for all samples in the 8-11 °C range. The catalysts employed in this study do not act as plasticizer and do not impact the thermal properties of the corresponding materials. The shear modulus in the rubbery state measured by frequency sweep analysis, showed only slight variation between materials with values between 0.26 MPa and 0.44 MPa (at T = 80°C). These results combined with swelling data and from the rubber elasticity theory,[35,36] confirmed that the network density of the PHU networks is not significantly affected by the catalysts or the occurrence of side reactions.

The mechanical properties of the PHU networks were then evaluated by tensile test experiments. As the experiments were performed at 25 °C, above the glass transition temperatures of the materials, the mechanical characteristics reported in Table 2 referred to the rubbery state of the materials. Hence, it is not surprising to obtain young modulus values with a magnitude order of the MPa. The slight differences observed can be related to slight difference of conversion or induced by urea formation already mentioned. In the case of PHU network prepared using *t*-BuOK as catalyst, a significant increase of mechanical properties was observed, the Young Modulus was roughly two times higher than that of the other samples. This behaviour was explained by the poor dispersion of the catalyst in the PHU matrix (and monomers) which can act as a solid charge in the crosslinked networks which improves the mechanical properties (see Figure S5). Overall and in agreement with the results observed via other characterization methods, there was no significant difference in thermoset properties between the different PHU samples. All analyses pointed out that the synthesis of cross-linked PHU network was effective and that the resulting properties were substantially independent of the catalyst employed during the preparation of the networks. The following dynamic evaluation is therefore not biased by the difference in structural or initial properties of the thermosets and is dictated only by the catalyst used.

Dynamic properties and exchange mechanism reactions

As mentioned in the introduction, PHU covalent dynamic exchanges are commonly admitted to occur *via* (i) transcarbamoylation (associative process) or (ii) retrocyclisation-aminolysis (dissociative process[37]). For instance, complete recovery of mechanical properties at moderate reprocessing temperature (80-120°C) were observed for DMAP-catalysed transcarbamoylation in previously reported PHU-CANs.[25] In order to determine accurately the mechanism involved in our systems, the dynamic properties of the PHU networks were assessed by rheological analyses (stress relaxation and frequency sweep experiments), reprocessing cycle tests, solubility tests (in 1,4-butanediol at 140°C) and model molecular studies. Surprisingly, almost all catalysts tested here, including DMAP were found to be inefficient to accelerate the exchange reaction. Normalized stress relaxation experiments (fitted with a stretch exponential) at 140°C presented in Figure 2.a, showed that DMAP, *p*-TSA or TU have similar characteristic relaxation times and profiles to the non-catalysed material. The tin-based Lewis acid DBTDL, was the only catalyst studied able to increase the dynamics of covalent exchange at 140°C ($\tau^*_{(DBTDL)} \approx 4\ 500$ s vs $\tau^*_{(NC)} \approx 47\ 000$ s). Stress relaxation tests performed at temperature between 130-160°C allowed to determine a flow activation energy $E_{A\,(DBTDL)}$ = 120 kJ.mol^{-1} (Figure 2b and S6) slightly higher than the values associated to the NC-networks ($E_{A\,(NC)}$ = 108 kJ.mol^{-1}, see Figure S7) and in the range of previously reported values.[24,28] Beta factor extracted from stretched exponential, also highlighted different distribution/complexity of relaxation mode between DBTDL and the other catalysts. While PHU prepared with other catalysts exhibited beta factor values (at 140°C) between 0.54 and 0.66 associated with complex relaxation mode, PHU-DBTDL beta factor was 0,89 (at 140°C) closer to a single relaxation mode ($\beta = 1$). Reducing the amount of DBTDL leads to an increase of characteristic relaxation time from $\tau^*_{(DBTDL\text{-}2mol\%)} \approx 4\ 500$ s to respectively vs $\tau^*_{(DBTDL\text{-}1mol\%)} \approx 1.3 \times 10^4$ s and $\tau^*_{(DBTDL\text{-}0.5mol\%)} \approx 25 \times 10^4$ s for PHU containing 1 and 0.5 mol% of catalyst as compare to hydroxyurethane groups (Figure 2c).

Frequency sweep experiments performed at temperature between 80 and 160°C, also highlighted different shear modulus evolution upon heating, depending on the catalyst used (Figure 3). DBTDL-based networks shear modulus was stable with an increasing temperature (Figure 3.a). In contrast, for the material obtained with the other catalysts or in the NC-material (representative curve in Figure 3.b), the shear modulus tended to decrease as the temperature rose. These results suggest a more pronounced dissociative pathway for samples prepared with other catalysts than DBTDL.[38] The ATR-IR spectra of DMAP-PHU networks after frequency sweep experiments (30 min at each temperature) presented in Figure S8 showed the characteristic vibrations bands $\nu_{C=O}$ of carbonate, urea and $\delta_{N\text{-}H}$ of primary amine with increasing intensity, thus confirming the retroformation of primary amine and cyclic carbonate and the occurrence of side reactions (urea bonds, see Scheme 2.c) during the temperature treatment. ATR-IR analysis of DBTDL-PHU networks performed at 140°C (1 spectrum/10 min) show no evolution of characteristic carbonyl vibration bands in the same region (Figure S9). The dissociative mechanism cannot be ruled out for DBTDL-PHU networks as cyclic carbonate $\nu_{C=O}$ was detected in ATR-IR after 3 reprocessing experiments (each of 8h at 120°C) but could be less predominant than for the other catalysts employed (Figure S10.d).

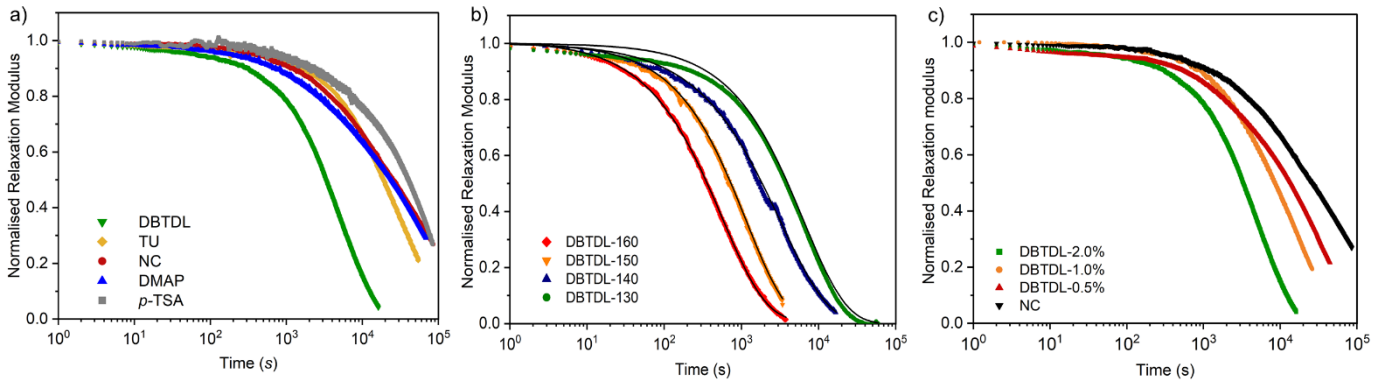

Figure 2. Stress relaxation experiments (parallel plate, d= 8 mm) of a) PHU-CANs prepared with selected catalysts (5 mol % at 140 °C) and b) PHU-CANs with DBTDL catalyst (2% mol) 130 °C, 140 °C, 150 °C and 160 °C (curves fitted with stretched exponential) c) PHU-CANs with DBTDL catalyst at 140°C and various catalyst amount (2%, 1% and 0,5% mol) compare to PHU-NC. β factor range between 0.86-0.91 for PHU-DBTDL and between 0.54 and 0.66 for the other catalysts employed or in the non-catalysed material.

The same tendency was observed in dissolution tests performed in 1,4 butanediol at 140°C for one week (Table S1). After only a few hours, DBTDL-based networks were solubilized while all the other materials tested remained insoluble (even after one week at 140°C) and exhibited roughly the same swelling ratio and gel content between them (Table S1). Finally, The DBTDL-PHU network was subjected to three consecutive reprocessing cycles (each of 8h at 120°C, 3 tons of pressure) and showed, despite a slight decrease of mechanical properties (measured by tensile test experiments), good reprocessability (Figure S10). The decrease of the mechanical properties recorded after each cycle was attributed to the formation of ureas and cyclic carbonates which reduce the crosslink density (Figure S10.d). Swelling experiments of the three times-reprocessed sample (in DMF at 80°C for 24h) also showed a higher swelling index of 255 ± 5 % and lower gel content 75% compare to the pristine PHU-DBTDL (Swelling index = 226 ± 2 and 86% of gel content) thus confirming a reduced crosslink density. The typical pictures of the DBTDL-catalysed and NC materials, presented in Figure S11 (after 24h at 140°C under 3 tons at the hot press), underlines the poor reprocessability which was observed for all other catalyst candidates under these conditions. Rheological properties, *i.e.* stress relaxation and frequency sweep, and ATR-IR analysis (at high temperature, Figure S8 and S9) also indicated that solely PHU containing the organometallic Lewis acid DBTDL effectively performed associative transcarbamoylation. The dynamic properties observed with the other catalysed PHU CANs are likely caused by dissociative transcarbamoylation exchange through the retro-formation of the cyclic carbonate and the amine functions, which is prone to irreversible urea formation. This combination of data reflects the low efficiency of catalysts, yet reported to be active in similar system, towards transcarbamoylation and prompted us to investigate different molecular model reactions.

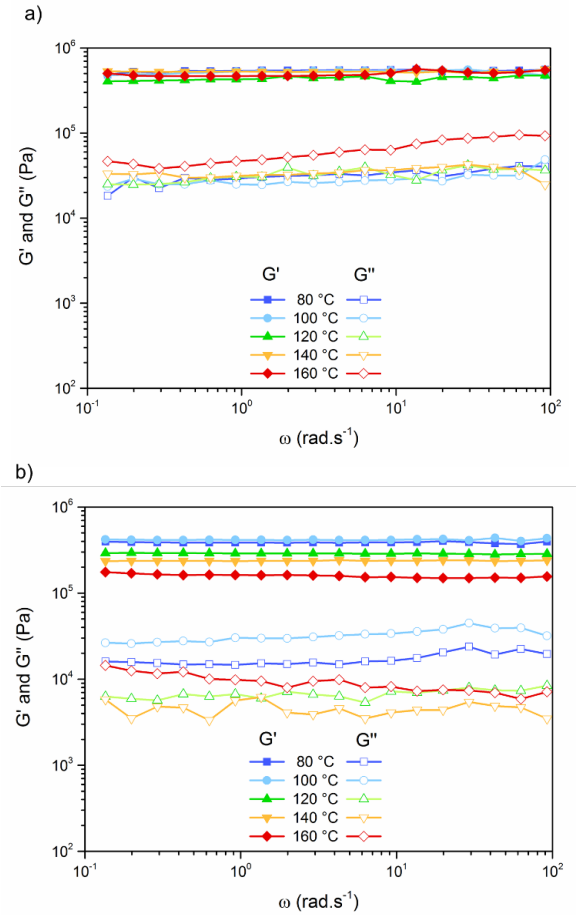

Molecular investigation of the catalyst on exchange mechanism reactions

The addition-elimination mechanism of asymmetric cyclic carbonate with primary amine yields hydroxy urethane moieties bearing either a primary or a secondary alcohol. As the nature, *i.e.* the steric hindrance, of alcohol is expected to have a large impact on their transcarbamoylation reactivity, this dependency was investigated using two model molecular reactions for: (i) aminolysis, and (ii) exchange reactions. Based on previous spectroscopic studies,[39] the relative abundance of primary and secondary alcohols groups was estimated by studying by ^{1}H NMR spectroscopy the reaction between TMPTC (trifunctional 5-CC used in this study) and *n*-butyl amine (3 equivalents) at

80°C during 24h and in presence of each of the studied catalyst (5 mol %) (Scheme 3.a). Diagnostic signals at 4.90 and 4.00 ppm of the primary and secondary alcohol moieties respectively were used to calculate the relative proportion of each isomer (Figure S12, S13 and Table 3). Regardless of the catalyst used, secondary alcohols were favoured with relative proportion above 67% (and up to 84%). In addition, the catalyst nature (acid or base) had only a low impact on the proportion without specific trend.

Following this result and to determine the influence of the alcohol hindrance on transcarbamoylation, hexanol and 2-heptanol were used as primary and secondary model alcohol respectively (Scheme 3.b). 2-Hydroxyethyl butyl carbamate, the hydroxy carbamate model molecule, was prepared by reacting butyl amine and ethylene carbonate (60°C for 24h). The model reactions were carried out in bulk at 140°C using 2-hydroxyethyl butyl carbamate, five equivalents of either primary or secondary alcohol and 5 mol% catalyst (as compared to carbamate groups, 2 mol% for DBTDL). ^{1}H NMR analysis (representative kinetics presented in Figure 4) allowed to measure both conversion (using ethylene glycol signal at 3.7 ppm, Figure 5.a) and the reactant/product/urea proportions (Figure 5.b). Model transcarbamoylation performed without catalyst or in the presence of *p*-TSA or TU, with either a primary or a secondary alcohol showed that no transcarbamoylation (associative or dissociative) occurred in these conditions (Figure 5.a, Table 3). In contrast, DMAP, DBTDL and *t*-BuOK were efficient catalysts for transcarbamoylation induced by primary alcohol. High conversions (80-100%) after 72h at 140°C were measured by ^{1}H NMR spectroscopy (Figure 5.a). In the case of DMAP, switching from a primary to a secondary alcohol drastically decreased the conversion (below 20% after 72h at 140°C). In contrast, DBTDL

reach almost similar conversion with primary or secondary alcohol. Potassium *tert*-butoxide showed intermediate decrease in reactivity.

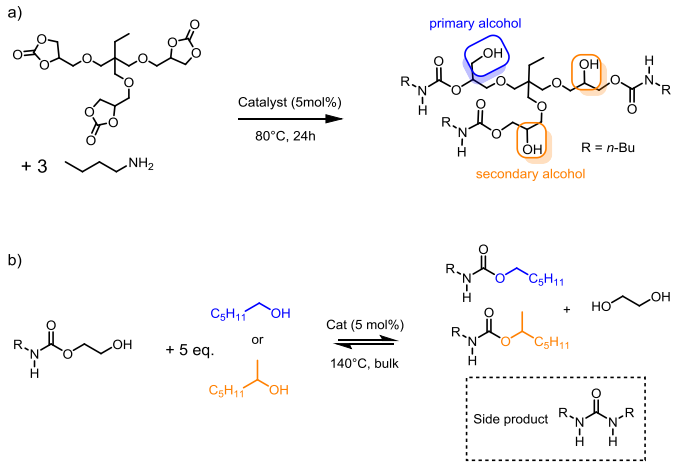

Scheme 3. a) Model reaction of trimethylolpropane tricarbonate with 3 equivalents of *n*-butyl amine (at 80°C for 24h) to determine the proportion of primary and secondary alcohol generated by the aminolysis of the studied carbonate monomer with various catalysts b) Transcarbamoylation reaction of 2-hydroxyethyl butylcarbamate with primary (hexanol) and secondary alcohol (2-heptanol) in bulk with various catalysts at 140°C.

The drop of reactivity observed in model transcarbamoylation catalysed by DMAP, *i.e.* using a secondary alcohol instead of a primary one, could explain the discrepancy of dynamic properties as compared to the previously reported PHU-DMAP covalent adaptable networks from 5-CC monomers.[20,25] Kinetics results on model molecules demonstrated that transcarbamoylation in DMAP/secondary alcohols system was slow and unselective (urea formation). As the proportions between primary and secondary alcohols were not determined in other reported systems, one might suspect that primary alcohol content can vary depending on the selected amine/cyclic carbonate system, and were presumably higher than the one measured herein. Alternatively, the chemical structure of 5-CC monomer was also put forward to explain the poor reprocessability observed using carbonated sorbitol-based monomer to prepare PHU-CAN catalysed by DMAP.[25] The authors suggested that the spatial proximity between cyclic carbonate moieties leads to the formation of a network with a higher crosslinked density and reduced chain mobility. A similar assumption can be made for TMPTC-based networks and explain the poor results (stress relaxation and reprocessing) observed for such system with DMAP catalyst.

Table 3. Catalyst-dependent proportions of primary and secondary alcohol in model TMPTC/*n*-butyl amine reaction (TMPTC/*n*-BuNH_2 = 1/3, at 80°C for 24h). Catalyst-dependent conversion and urea content for the transcarbamoylation of 2-hydroxyethyl butyl carbamate (1 eq.) with hexanol (5 eq.) or 2-heptanol (5 eq.) in at 140°C.

Catalyst	I/II alcohol (%)[a]	% conv. (I)[b]	% conv. (II)[c]	Product/ Urea (I)[b]	Product/ Urea (II)[c]
NC	33/67	3	1	*n.d.*	*n.d.*
t-BuOK	28/72	100	65	81/17	30/35
TBD	17/83	90	84	83/7	39/45
TU	20/80	≤ 1%	≤ 1%	*n.d.*	*n.d.*
DBU	26/74	80	57	47/33	17/40
DBTDL[d]	21/79	85	73	77/6	73/6
DMAP	16/84	80	17	64/16	6/11
p-TSA	19/81	5	3	*n.d.*	*n.d.*

Determined by ^{1}H NMR spectroscopy in $CDCl_3$ a) after 24h at 80°C in bulk b) after 72h at 140°C in bulk using hexanol (5eq) c) after 72h at 140°C in bulk using 2-heptanol (5eq) d) DBTDL was used at 2 mol% to [TMPTC]. *n.d. = not determined*

According to model molecular reaction results, *t*-BuOK appears as a promising candidate to promote transcarbamoylation in PHU-networks. However, material characterizations (rheology) demonstrated only poor dynamic properties for the PHU-*t*-BuOK material. This behaviour was explained by the unsatisfactory dispersion of the catalyst in the PHU matrix (already mentioned above in the tensile test experiments) despite the dissolution/dispersion of this catalyst in DCM or THF prior to the materials synthesis. Looking at the relative proportions of reactant/product/urea monitored by ^{1}H NMR spectroscopy (Figure 5.b), variations also appeared between the three most active catalysts (DMAP, DBTDL and *t*-BuOK). Relatively high urea content (16-20 mol%) were measured for the model reactions catalysed by DMAP and *t*-BuOK with 1-hexanol. When 2-heptanol was used, the urea content quantified was even higher than that of the desired transcarbamoylation product, highlighting the occurrence of side reactions. Urea formation is admitted to occur in a two-step process with: (1) retro-formation of primary amine and cyclic carbonate, and (2) nucleophilic attack of a primary amine on a urethane group. In contrast, employing hexanol leads to a rapid conversion of 2-hydroxyethyl butyl carbamate into hexyl butyl

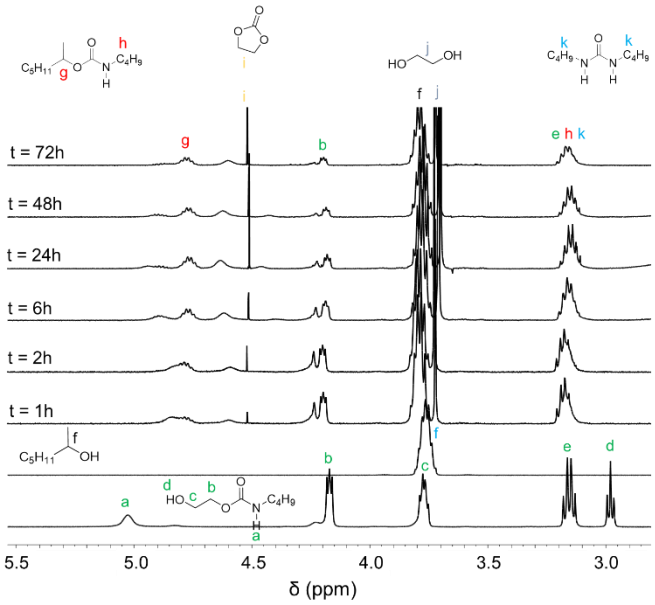

Figure 4. ^{1}H NMR spectra (in $CDCl_3$) of the transcarbamoylation of 2-hydroxyethyl butyl carbamate by 2-heptanol in bulk with DBTDL at 140°C at different reaction time.

carbamate thus avoiding the retroformation of cyclic carbonate and urea formation. Surprisingly, only urea signals were detected in ^{1}H NMR spectra whereas the signal of ethylene carbonate (singlet at 4.55 ppm) was either non-detected or of low intensity (although it should be equal to the amount of urea formed), thus suggesting that cyclic carbonate was consumed presumably by reaction with the alcohol in excess under these conditions (5 equivalents of alcohol, 140°C). This was confirmed by a control experiment (ethylene carbonate (1 eq.), 2-heptanol (5 eq.), *t*-BuOK (5 mol%)) which showed the characteristic ^{1}H NMR signal of ethylene glycol (Figure S15).

Discussion on catalyst-dependent exchange mechanism

By combining molecular and macromolecular characterisations, we suggested a catalyst-dependent transcarbamoylation mechanism occurring in PHU-CAN depicted in Scheme 4. The dissociative mechanism, involving the retroformation of 5-CC and primary amine, seems to be predominant when secondary alcohol (major product of aminolysis) are presents (Scheme 4.a). Depending on the catalyst employed, two different behaviours were observed. When strong bases (DMAP, t-BuOK, DBU or TBD) were employed, the generation of primary amine in presence of these catalysts leads to urea formation detected in both molecular (by ^{1}H NMR spectroscopy) and material analysis (ATR-IR spectroscopy). This phenomenon could be explained either by the activation of primary amine by strong bases but also *via* activation of carbamate moieties which has been already reported in the literature for TBD-catalysed polyurea synthesis.[33] Surprisingly, acidic or electrophilic catalysts such *p*-TSA and thiourea showed no activity in model transcarbamoylation reactions while rheological characterisations (frequency sweep and stress relaxation) proved that dissociative covalent exchanges took place. These catalysts also limited the occurrence of side reaction as no urea functions have been detected by ^{1}H NMR spectroscopy or ATR-IR analysis (Figure S16). The selective activation of heterocyclic carbonyl moieties, known in lactone ring-opening polymerisation,[40,41] was put forward in Scheme 4a to explain why aminolysis was favoured in this case. These assumptions and the rationalisation of the catalyst effect needs to be further supported by both theoretical (DFT calculation) and experimental data.

In the particular case of DBTDL, the reactivity was not affected by the alcohol nature and material properties (shear modulus stable at high temperature, dissolution test and faster relaxation) prompt us to suggest an alternative exchange mechanism. Organotin compounds are known to activate both alcohol and carbamate moieties through a coordinated transition state.[42] The coordinated mechanism suggested in Scheme 4b, which involved a coordination of alcohol (regardless of the alcohol nature) and carbamate could explain the differences observed between DBTDL and the other catalysts used in this study.

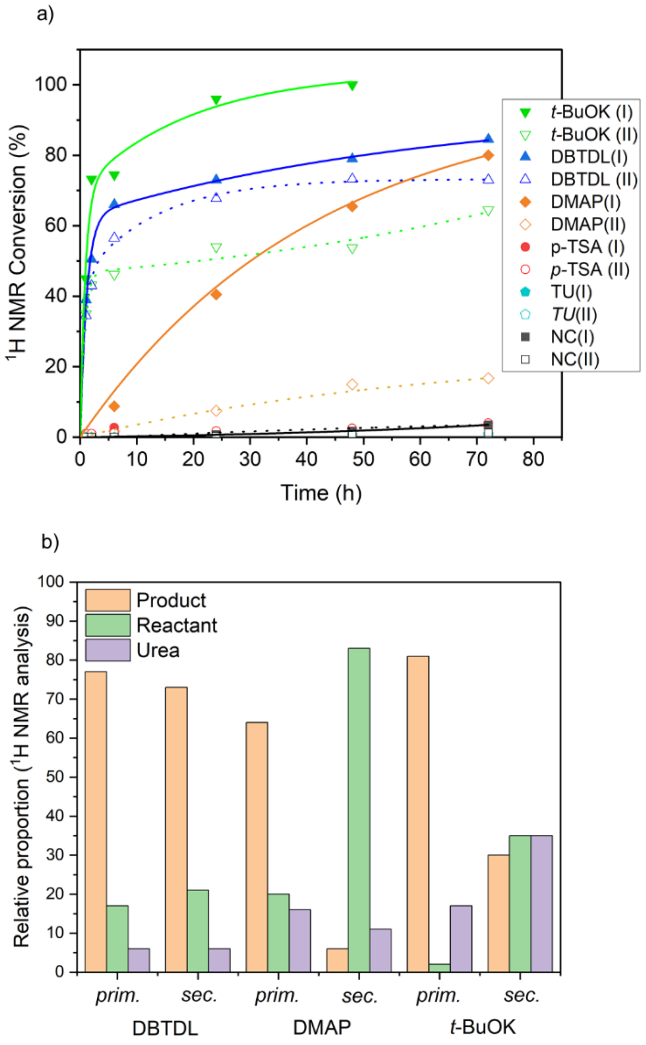

Figure 5. a) ^{1}H NMR conversion of model compound 2-hydroxyethyl butyl carbamate as a function of time depending on the alcohol (hexanol (*prim*) in straight line and 2-heptanol (*sec*) in dotted line) and catalyst (140°C, 5 mol%; apart DBTDL at 2 mol%) b) Relative proportions of 2-hydroxyethyl butyl carbamate (reactant in green), hexyl butyl carbamate (product in orange) and di-*n*-butyl urea (urea in purple) as a function of alcohol and catalyst (72h, 140°C, 5 mol%).

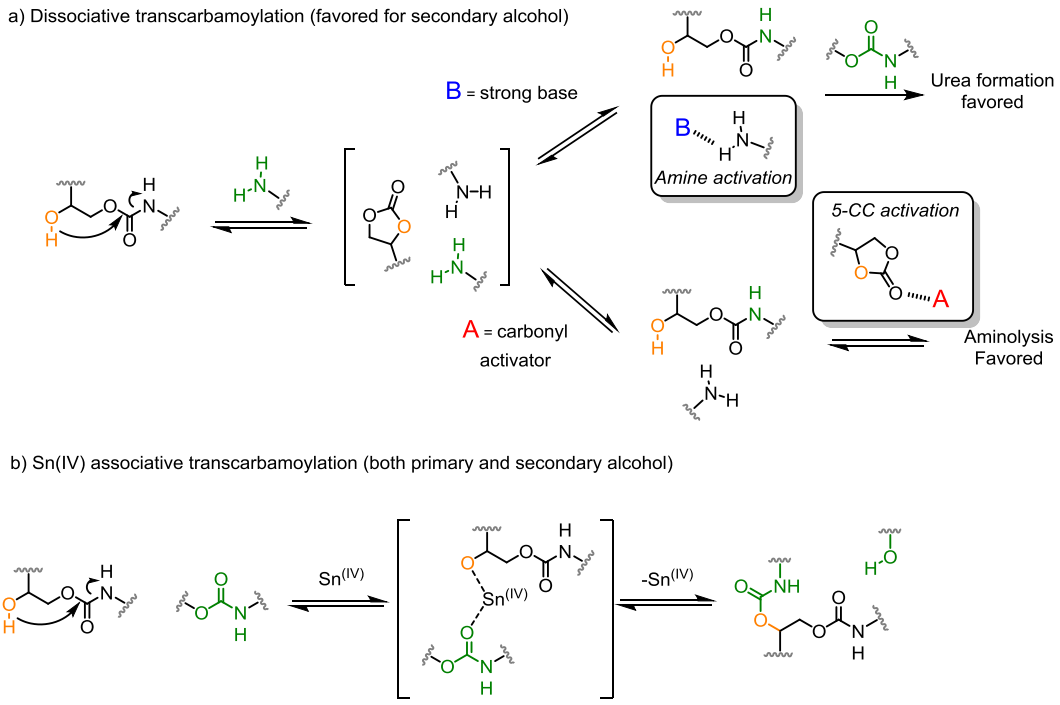

Scheme 4. Suggested mechanism for transcarbamoylation in PHU-CANs containing different catalysts *via* a) dissociative transition state with secondary alcohol and b) coordinated transition state with both primary and secondary alcohol for DBTDL-catalysed ($Sn^{(IV)}$) associative transcarbamoylation

Conclusion

Herein we explored and rationalized the activity of different catalysts for the preparation of polyhydroxyurethane covalent adaptable networks. Strong base catalysts (TBD or DBU) induced urea formation right from the polymerisation step (aminolysis of 5-member cyclic carbonate). Selected PHU networks were fully characterized using thermo-mechanical analysis (TGA, DSC and tensile test), rheology experiments (stress relaxation, frequency sweep), spectroscopy (ATR-IR), as well as swelling and reprocessing tests. In summary, model molecular reactions confirmed that DBTDL is the only compound able to catalyse transcarbamoylation with both primary/secondary alcohol and limited side reactions at the same time. By combining molecular and macromolecular characterizations, the present investigations also explain the differences observed between DBTDL and the previously reported PHU covalent adaptable networks, and especially those based on DMAP as catalyst. The proportion of primary and secondary alcohols seemed to play a prominent role in controlling the dynamic properties of PHU-CAN and should be one of the major concerns (with the catalyst choice) when designing such systems. Increasing the primary alcohol content in PHU networks could offer better and faster reprocessability of PHU-CANs, thus limiting side reactions and expanding the scope of catalyst candidates. More sustainable and benign catalysts known to be active in PU transcarbamoylation should be also employed for "greener" PHU-CAN design.[30]

Materials and methods

Chemicals. TMPTC [43] and thiourea [44] catalyst were prepared according to the literature. 4,9-Dioxa-1,12-dodecanediamine (99% Sigma Aldrich), ethylene carbonate (98%, Sigma Aldrich), n-butyl amine (99.5%, Sigma Aldrich), *p*-toluene sulfonyl acid (*p*-TSA, 95% Alfa Aesar), 1,5,7-triazabicyclo[4.4.0]dec-5-ene (TBD, 98% TCI), 1,8-diazabicyclo[5.4.0]undec-7-ene (DBU, 98% Sigma Aldrich), potassium *tert*-butoxide (*t*-BuOK, ≥ 98% Sigma Aldrich), 4-(dimethylamino) pyridine (DMAP, 99% Sigma Aldrich), dibutyltin(IV)dilaurate, (DBTDL, 95% Sigma Aldrich), Dichloromethane (DCM, Carlos Erba) were used as received.

Model Reactions experiments. *Synthesis of 2-hydroxyethyl butyl carbamate.* In a 50 mL round-bottom flask equipped with a magnetic stirrer, were added 10 g (1eq., 0.114 mol) of ethylene carbonate and 9.97 g (1.2 eq., 0.136 mol) of *n*-butyl amine at room temperature. The reaction mixture was kept under stirring at 60°C for 24h. The crude product was purified on flash chromatographic column (ethyl acetate 100% as eluent) and 18.0 g of viscous oil was recovered (yield = 90%).
^{1}H NMR (CDCl$_3$, 298 K, 400 MHz) δ (ppm) = 5.03 (broad, 1H, N*H*(carbamate)); 4.17 (t, 2H, C*H*$_2$-CH$_2$-OH, J = 4.4 Hz); 3.77 (m, 2H, CH$_2$-C*H*$_2$-OH); 3.15 (q, 2H, C*H2*-NH, J= 7.2 Hz); 2.98 (t, 1H, -O*H*, J= 5.6 Hz); 1.46 (m, 2H, CH$_2$); 1.33 (m, 2H, CH$_2$); 0.90 (t, 3H, CH$_3$, J = 7.5 Hz).
Aminolysis of TMPTC.
In a 5 mL vial were introduced 1.0 g (CEW = 180 g.eq^{-1}, 5.55 mmol of carbonate functions) of TMPTC, followed by 402 mg of *n*-butylamine (1 eq, 5.55 mmol) and catalysts (0.27 mmol, 0.05 eq as compared to the carbonate groups). The reaction mixture was stirred and heated at 80 °C for 24 hours. ^{1}H NMR analysis of isomer content (in the crude product) is presented in Figure S11.
Transcarbamoylation model reaction. In a haemolysis tube were introduced 1.0 g (6.21 mmol, 1 eq) of 2-hydroxyethyl butyl carbamate, 3.87 mL (31.05 mmol, 5 eq) of 1-hexanol and catalysts (0.31 mmol, 0.05 eq as compared to the carbonate groups). The reaction mixture was stirred and heated at 140ºC for 72 h. Aliquots were taken at different time (0, 1 h, 2 h, 6 h, 24 h, 48 h, 72 h) and the crude product was analysed by ^{1}H NMR spectroscopy in CDCl$_3$. Conversions were calculated using the appearance of ethylene glycol signal (singlet at 3.70 ppm).
PHU networks synthesis. In a typical experiment, 10 g of TMPTC (CEW = 180 g. eq^{-1}; 55.5 mmol of carbonate functions) and 5.73 g (1.01 eq., 56.1 mmol of NH$_2$) of 4,9-dioxa-1,12-dodecanediamine were added in a polypropylene 50 mL container. A solution containing 2.7 mmol (5 mol% as compared to carbonate functions) of catalyst dissolved in DCM (4 mL) was then added to the mixture and stirred at 2500 rpm for 5 min at RT using a speed mixer. DCM was used to ensure both good dispersion of the catalyst and monomer mixing as TMPTC is highly viscous at room temperature. The mixture was then casted on a PTFE mould, degassed under vacuum for 10 min at 25°C

and put in an oven at 80°C for 24h. Complete conversion of carbonate groups was checked by ATR-IR spectroscopy.

Nuclear Magnetic Resonance. Nuclear Magnetic Resonance experiments were carried out in deuterated solvents using a Bruker Avance III 400 MHz NMR spectrometer at 298K.

Titration of the carbonate equivalent weight by ^{1}H-NMR. The Carbonate Equivalent Weight (CEW) is the amount of product needed for one equivalent of reactive carbonate function. It was determined by ^{1}H-NMR using an internal standard (benzophenone). A known mass of product and benzophenone was poured into an NMR tube and 500 µL of $CDCl_3$ were added. The CEW was determined using equation (1) by comparing the integration values of the peak corresponding to the benzophenone protons (7.5–7.8 ppm) with those of the cyclic carbonate moiety protons (4.81 ppm). The measurement of the CEW was performed in triplicate.

Equation 1 $$CEW = \frac{\int PhCOPh * H_{carbonate}}{\int carboante * H_{PhCOPh}} * \frac{m_{carbonate}}{m_{PhCOPh}} * M_{PhCOPh}$$

$\int_{PhCOPh}$: integral of the signal from benzophenone protons; $\int_{carbonate}$: integral of the signals from protons in α of the carbonate function; the integration value of the signal from protons in α of the carbonate function; $H_{carbonate}$: the number of protons in α of the carbonate function; H_{PhCOPh}: the number of benzophenone protons; $m_{carbonate}$: the product mass; m_{PhCOPh}: the benzophenone mass and M_{PhCOPh}: the benzophenone molecular weight.

Fourier Transform Infrared Spectroscopy. Infrared (IR) spectra were recorded on a Nicolet 210 Fourier transform infrared (FTIR) spectrometer equipped with a Specac golden gate attenuated total reflection (ATR) heating cell. The characteristic IR absorptions mentioned in the text are reported in cm^{-1}.

Thermogravimetric Analyses. Thermogravimetric Analyses (TGA) were carried out using TG 209F1 apparatus (Netzch). Approximately 10 mg of sample were placed in an aluminium crucible and heated from room temperature to 580 °C at a heating rate of 20 °C/min under nitrogen atmosphere (60 mL/min).

Differential Scanning Calorimetry. Differential Scanning Calorimetry (DSC) analyses were carried out using a NETZSCH DSC200F3 calorimeter, which was calibrated using indium, *n*-octadecane and *n*-octane standards. Nitrogen was used as purge gas. Approximately 10 mg of sample were placed in a perforated aluminium pan and the heat exchanges were recorded between -150 °C and 150 °C at 20 °C/min to observe the glass transition temperature. The T_g values were measured on the second heating ramp to erase the thermal history of the polymer. All the reported characteristic temperatures are average values of three measurements.

Rheology experiments. Rheology experiments were performed on a ThermoScientific Haake Mars 60 rheometer equipped with a lower electrical temperature module and an active upper heating system, with a textured 8-mm plane-plane geometry. For all rheology experiments, the applied stress was comprised in the linear viscoelastic region (checked by amplitude sweep experiments at 140°C and 80 °C). A 5 N axial force was applied to ensure proper contact between the plates and the samples for all experiments. Each sample was only used for one analysis in order to get easily reproducible results. For stress-relaxation experiments, a constant 3 % shear strain was applied on samples, and the relaxation modulus evolution with time was monitored at different isotherms. The obtained (from stretched exponential fitting) characteristic relaxation time τ was used to calculate the activation energy (Arrhenius plot). The reproducibility of the analysis has been verified for at least one temperature for each sample for the stress-relaxation measurements. For frequency sweep experiments, a 1 % shear strain was applied for frequencies going from 0.1 $rad.s^{-1}$ to 50 $rad.s^{-1}$.

Swelling index and solubility test. Three samples from the same material, of around 20 mg each, were separately immersed in DMF at 80°C for 24 h. The swelling index (SI) was calculated using Equation 2, where m_2 is the mass of the swollen material and m_1 is the initial mass. Reported swelling index are average values of the three samples. The same procedure was followed for solubility tests of PHU-CANs by immersing samples in butanediol at 140°C for 1 week.

Equation 2 $$SI = \frac{m_2 - m_1}{m_1} \times 100$$

Gel content. Three samples from the same material, of around 200 mg each, were separately immersed in DMF for 24 h. The samples were then dried in a ventilated oven at 110 °C for 24 h. The gel content (GC) was calculated using Equation 3, where m_3 is the mass of the dried material and m_1 is the initial mass. Reported gel content are average values of the three samples.

Equation 3 $$GC = \frac{m_3}{m_1} \times 100$$

Tensile test. Tensile tests were performed at room temperature on at least three different dog-bone specimens of 4 mm width, 25 mm gauge length, and ≈ 2 mm thickness. All tensile tests were performed with an Instron 5900 machine at a deformation rate of 5 $mm.min^{-1}$.

Conflicts of interest

The authors declare no conflicts of interest.

References

1 J. R. Jambeck, R. Geyer, C. Wilcox, T. R. Siegler, M. Perryman, A. Andrady, R. Narayan and K. L. Law, *Science*, 2015, **347**, 768–771.
2 T. Stanton, P. Kay, M. Johnson, F. K. S. Chan, R. L. Gomes, J. Hughes, W. Meredith, H. G. Orr, C. E. Snape, M. Taylor, J. Weeks, H. Wood and Y. Xu, *WIREs Water*, , DOI:10.1002/wat2.1490.
3 G. W. Coates and Y. D. Y. L. Getzler, *Nat. Rev. Mater.*, 2020, **5**, 501–516.
4 D. J. Fortman, J. P. Brutman, G. X. De Hoe, R. L. Snyder, W. R. Dichtel and M. A. Hillmyer, *ACS Sustain. Chem. Eng.*, 2018, **6**, 11145–11159.
5 C. Jehanno, J. W. Alty, M. Roosen, S. De Meester, A. P. Dove, E. Y.-X. Chen, F. A. Leibfarth and H. Sardon, *Nature*, 2022, **603**, 803–814.
6 F. M. Haque, J. S. A. Ishibashi, C. A. L. Lidston, H. Shao, F. S. Bates, A. B. Chang, G. W. Coates, C. J. Cramer, P. J. Dauenhauer, W. R. Dichtel, C. J. Ellison, E. A. Gormong, L. S. Hamachi, T. R. Hoye, M. Jin, J. A. Kalow, H. J. Kim, G. Kumar, C. J. LaSalle, S. Liffland, B. M. Lipinski, Y. Pang, R. Parveen, X. Peng, Y. Popowski, E. A. Prebihalo, Y. Reddi, T. M. Reineke, D. T. Sheppard, J. L. Swartz, W. B. Tolman, B. Vlaisavljevich, J. Wissinger, S. Xu and M. A. Hillmyer, *Chem. Rev.*, 2022, **122**, 6322–6373.
7 D. Bello, C. A. Herrick, T. J. Smith, S. R. Woskie, R. P. Streicher, M. R. Cullen, Y. Liu and C. A. Redlich, *Environ. Health Perspect.*, 2007, **115**, 328–335.
8 OECD, *Global Plastics Outlook: Economic Drivers, Environmental Impacts and Policy Options*, OECD, 2022.
9 Z. S.Petrovic, J. Ferguson, *Progr. Polym. Sci*. **1991**, 16, 695−836.
10 L. Maisonneuve, O. Lamarzelle, E. Rix, E. Grau and H. Cramail, *Chem. Rev.*, 2015, **115**, 12407–12439.
11 E. Delebecq, J.-P. Pascault, B. Boutevin and F. Ganachaud, *Chem. Rev.*, 2013, **113**, 80–118.
12 B. Blattmann, M. Fleischer, M. Bähr, R. Mülhaupt, *Macromol. Rapid Commun.*, **2014**, 35, 1238−1254.
13 N. Yadav, F. Seidi, D. Crespy and V. D'Elia, *ChemSusChem*, 2019, **12**, 724–754.
14 F. D. Bobbink, A. P. van Muyden and P. J. Dyson, *Chem. Commun.*, 2019, **55**, 1360–1373.
15 B. Grignard, S. Gennen, C. Jérôme, A. W. Kleij and C. Detrembleur, *Chem. Soc. Rev.*, 2019, **48**, 4466–4514.
16 M. Blain, A. Cornille, B. Boutevin, R. Auvergne, D. Benazet, B. Andrioletti and S. Caillol, *J. Appl. Polym. Sci.*, 2017, **134**, 44958.
17 A. Cornille, M. Blain, R. Auvergne, B. Andrioletti, B. Boutevin and S. Caillol, *Polym. Chem.*, 2017, **8**, 592–604.
18 A. Yuen, A. Bossion, E. Gómez-Bengoa, F. Ruipérez, M. Isik, J. L. Hedrick, D. Mecerreyes, Y. Y. Yang and H. Sardon, *Polym. Chem.*, 2016, **7**, 2105–2111.
19 T. Tomita, F. Sanda, T. Endo, *J. Polym. Sci. Part A*, **2011**, 39,860–867.
20 C. Bakkali-Hassani, D. Berne, V. Ladmiral and S. Caillol, *Macromolecules*, 2022, **55**, 7974–7991.
21 X. Chen, L. Li, K. Jin and J. M. Torkelson, *Polym Chem*, 2017, **8**, 6349–6355.
22 D. J. Fortman, J. P. Brutman, M. A. Hillmyer and W. R. Dichtel, *J. Appl. Polym. Sci.*, 2017, **134**, 44984.
23 D. J. Fortman, J. P. Brutman, C. J. Cramer, M. A. Hillmyer and W. R. Dichtel, *J. Am. Chem. Soc.*, 2015, **137**, 14019–14022.
24 A. Hernández, H. A. Houck, F. Elizalde, M. Guerre, H. Sardon and F. E. Du Prez, *Eur. Polym. J.*, 2022, **168**, 111100.
25 X. Chen, L. Li and J. M. Torkelson, *Polymer*, 2019, **178**, 121604.
26 S. Hu, X. Chen and J. M. Torkelson, *ACS Sustain. Chem. Eng.*, 2019, **7**, 10025–10034.
27 X. Chen, L. Li, T. Wei, D. C. Venerus and J. M. Torkelson, *ACS Appl. Mater. Interfaces*, 2019, **11**, 2398–2407.

28 S. Hu, X. Chen, M. A. Bin Rusayyis, N. S. Purwanto and J. M. Torkelson, *Polymer*, 2022, **252**, 124971.
29 F. Elizalde, R. H. Aguirresarobe, A. Gonzalez and H. Sardon, *Polym. Chem.*, 2020, **11**, 5386–5396.
30 D. J. Fortman, D. T. Sheppard and W. R. Dichtel, *Macromolecules*, 2019, **52**, 6330–6335.
31 S. Tshepelevitsh, A. Kütt, M. Lõkov, I. Kaljurand, J. Saame, A. Heering, P. G. Plieger, R. Vianello and I. Leito, *Eur. J. Org. Chem.*, 2019, **2019**, 6735–6748.
32 A. Bossion, R. H. Aguirresarobe, L. Irusta, D. Taton, H. Cramail, E. Grau, D. Mecerreyes, C. Su, G. Liu, A. J. Müller and H. Sardon, *Macromolecules*, 2018, **51**, 5556–5566.
33 S. Ma, C. Liu, R. J. Sablong, B. A. J. Noordover, E. J. M. Hensen, R. A. T. M. Van Benthem and C. E. Koning, *ACS Catal.*, 2016, **6**, 6883–6891.
33 https://organicchemistrydata.org/hansreich/resources/pka/pka_data/pka-compilation-williams.pdf
34 J. D. Ferry, Viscoelastic Properties of Polymers Ed. John Wiley & Sons, 1980, ISBN : 0-471-04894-1
36 P. J. Flory and J. Rehner, *J. Chem. Phys.*, 1943, **11**, 521–526.
37 A. Gomez-Lopez, F. Elizalde, I. Calvo and H. Sardon, *Chem. Commun.*, 2021, **57**, 12254–12265.
38 A. Jourdain, R. Asbai, O. Anaya, M. M. Chehimi, E. Drockenmuller and D. Montarnal, *Macromolecules*, 2020, **53**, 1884–1900.
39 J. L. J. van Velthoven, L. Gootjes, D. S. van Es, B. A. J. Noordover and J. Meuldijk, *Eur. Polym. J.*, 2015, **70**, 125–135.
40 X. Zhang, G. O. Jones, J. L. Hedrick and R. M. Waymouth, *Nat. Chem.*, 2016, **8**, 1047–1053.
41 A. Chuma, H. W. Horn, W. C. Swope, R. C. Pratt, L. Zhang, B. G. G. Lohmeijer, C. G. Wade, R. M. Waymouth, J. L. Hedrick and J. E. Rice, *J. Am. Chem. Soc.*, 2008, **130**, 6749–6754.
42 J. P. Brutman, D. J. Fortman, G. X. De Hoe, W. R. Dichtel and M. A. Hillmyer, *J. Phys. Chem. B*, 2019, **123**, 1432–1441.
43 H. Matsukizono and T. Endo, *J. Mater. Sci. Res.*, 2016, **5**, 11.
44 R. C. Pratt, B. G. G. Lohmeijer, D. A. Long, P. N. P. Lundberg, A. P. Dove, H. Li, C. G. Wade, R. M. Waymouth and J. L. Hedrick, *Macromolecules*, 2006, **39**, 7863–7871.